# Development of a low-temperature photoelectron spectroscopy instrument using an electrospray ion source and a cryogenically controlled ion trap

Xue-Bin Wang and Lai-Sheng Wang[a)]
*Department of Physics, Washington State University, 2710 University Drive, Richland, Washington 99354, USA*
*and Chemical and Materials Sciences Division, Pacific Northwest National Laboratory, MS 8-88, P.O. Box 999, Richland, Washington 99352, USA*

(Received 23 March 2008; accepted 20 June 2008; published online 17 July 2008)

The ability to control ion temperatures is critical for gas phase spectroscopy and has been a challenge in chemical physics. A low-temperature photoelectron spectroscopy instrument has been developed for the investigation of complex anions in the gas phase, including multiply charged anions, solvated species, and biological molecules. The new apparatus consists of an electrospray ionization source, a three dimensional (3D) Paul trap for ion accumulation and cooling, a time-of-flight mass spectrometer, and a magnetic-bottle photoelectron analyzer. A key feature of the new instrument is the capability to cool and tune ion temperatures from 10 to 350 K in the 3D Paul trap, which is attached to the cold head of a closed cycle helium refrigerator. Ion cooling is accomplished in the Paul trap via collisions with a background gas and has been demonstrated by observation of complete elimination of vibrational hot bands in photoelectron spectra of various anions ranging from small molecules to complex species. Further evidence of ion cooling is shown by the observation of $H_2$-physisorbed anions at low temperatures. Cold anions result in better resolved photoelectron spectra due to the elimination of vibrational hot bands and yield more accurate energetic and spectroscopic information. Temperature-dependent studies are made possible for weakly bonded molecular and solvated clusters, allowing thermodynamic information to be obtained. © *2008 American Institute of Physics.* [DOI: 10.1063/1.2957610]

## I. INTRODUCTION

Many important chemical reactions, including all biologically related processes, take place in an aqueous solution, where the complications of the bulk environments present considerable challenges for obtaining a molecular-level understanding of phenomena in the solution phase. Gas phase studies of solution phase species and their microsolvation by controlled solvent numbers allow their intrinsic properties to be obtained and provide ideal molecular models for the condensed phase environments. In the late 1990s, we developed an experimental technique combining electrospray ionization (ESI) and photoelectron spectroscopy (PES),[1] which was aimed at investigating solution phase species and chemistry in the gas phase.[2–4] Using this apparatus, we have carried out systematic investigations on a variety of subjects related to solution phase species and phenomena, including multiply charged anions,[2,5–9] solvation and solvent stabilization of complex anions,[3,4,10] inorganic metal complexes and redox species,[11–14] and biorelated systems.[15–20] The combination of ESI and PES has proven to be a general and powerful technique to probe solution phase species and chemistry in the gas phase. However, one of the limitations of the apparatus is the lack of ion temperature control because both the ion source and the ion accumulation device are operated at room temperature. Molecular species, particularly complex anions or weakly bonded species, can carry substantial internal energies even at room temperature. Consequently, significant thermal broadening can result, limiting the spectral resolution and accuracy of the obtained energetic information. In addition, unique and novel temperature-dependent phenomena, such as conformation changes for complex anions or isomer distributions for weakly bonded complexes, cannot be investigated. Therefore, some types of ion cooling and temperature control would greatly enhance the power of the ESI-PES technique to probe solution molecules and complex anions.

The ability to control ion temperatures is critical for gas phase spectroscopy in general and has been a real challenge in chemical physics. Supersonic expansion,[21,22] helium nanodroplet,[23–25] and argon tagging[26,27] have been used effectively to create cold molecules and ions for gas phase chemical dynamics and spectroscopy studies. However, precise temperature control and tuning over a wide temperature range have been extremely difficult and have not been accomplished. Recent advances in ion trap technology have made it possible to produce cold ions down to very low temperatures and to allow temperature tuning in principle.[28–30] The basic idea of ion cooling in a trap is to use a buffer gas as a thermal bath at a well-defined temperature and pressure. Ions in the trap are confined kinetically by a

[a)]Electronic mail: ls.wang@pnl.gov.

 

time-varying electric field and thermalized both internally and translationally via collisions with the buffer gas.

Here, we report the design and construction of a variable temperature PES instrument, which consists of an ESI source, a cryogenically controlled ion trap, a time-of-flight mass spectrometer (TOFMS), and a magnetic-bottle TOF photoelectron analyzer. The ion temperature control is accomplished using a three dimensional (3D) Paul trap, which is attached to the cold head of a closed cycle helium refrigerator capable of reaching down to 5 K. The temperature of the Paul trap can be controlled and tuned continuously from 10 to 350 K. In the next two sections, we describe the general considerations and details of the experimental design, followed by detailed characterizations of the new instrument in Sec. IV. We demonstrate ion cooling on the basis of elimination of vibrational hot bands in PES spectra and observation of physisorbed $H_2$-complexes. Weak molecular interactions and entropic effects are studied via temperature-dependent PES experiments.

## II. GENERAL CONSIDERATIONS

### A. Choice of low-temperature ion trap

Thermalization of hot ions by a buffer gas has been widely used in mass spectrometry.[31–34] Gerlich first demonstrated the feasibility of cooling molecular ions down to very low temperatures (a few kelvins) by thermalization with a helium buffer gas in a 22-pole ion trap,[28] which is attached to a cryogenically controlled helium refrigerator. The crucial cooling effects achieved in the 22-pole ion trap have been shown in ion molecule reactions,[29,30] cluster associations,[35] and, very recently, infrared spectroscopy.[36,37] Higher-order radio-frequency (rf) traps, such as the 22-pole trap, are preferred for ion cooling because of the flatness of the trapping potentials, which reduce rf heating. However, such high-order traps only confine ions radially and tend to yield larger trapping volumes both axially and radially. While such configurations are quite advantageous for *in situ* ion molecular reactions or IR spectroscopic studies followed by mass analyses using a quadruple mass filter,[28,29,35–37] it is rather inefficient in coupling the linear ion traps with a low repetition rate TOF mass analyzer, as dictated by our PES experiments,[1] due to difficulties in compressing ions in the axial direction.

On the other hand, a 3D Paul trap confines ions both axially and radially (like a point source) and is more suitable for coupling with a low repetition rate TOFMS, as demonstrated previously,[38,39] as well as in our previous room temperature ESI-PES apparatus.[1] However, the trapping potentials along both axial and radial directions are quadratic in the Paul trap and can thus potentially induce rf heating, making it unsuitable for ion cooling. Fortunately, it has been shown that when the Paul trap is operated at low $q$ values ($<0.3$), it is possible to avoid rf heating.[40] Indeed, Parks and co-workers demonstrated collisional relaxation and cooling effects of ions in a Paul trap attached to a liquid nitrogen cooled plate.[41,42] Additionally, the Paul trap is commercially available with all the rf power supplies and control electronics for a wide mass range, simplifying the design and construction. Consequently, we have chosen the 3D Paul trap as our ion trapping and cooling device, whose temperatures will be controlled by attaching it to the cold head of a closed cycle helium refrigerator, similar to the Gerlich 22-pole ion trapping and cooling device.[28]

### B. Addition of a quadruple mass filter for pretrapping mass detection and selection

In our previous ESI-PES apparatus,[1] we store all incoming ions from an ESI source in a 3D Paul trap. The design was relatively simple, but the trapping efficiency may be reduced, especially for weakly populated species, due to space charge effects in the ion trap. Thus, it would be desirable to have some kind of pretrapping mass selection. The addition of a quadruple mass filter between the ESI source and the ion trap would accomplish this goal, and it would also allow convenient detections of pristine ions coming from the ESI source. The latter could be very valuable because the process of loading ions into the ion trap may destroy weakly bonded species. Thus, independent knowledge of the pristine ions coming from the ESI source would be helpful in tuning the conditions of both the ESI source and the ion trap. Thus, in the new low-temperature instrument, a quadruple mass filter has been added, which can monitor ions produced from the ESI source before the ion trap and can also act as a pretrapping mass selector.

## III. DESCRIPTION OF THE INSTRUMENT

The overall layout and design of the new low-temperature ESI-PES apparatus is shown in Fig. 1. It consists of an ESI quadruple mass spectrometry (QMS) system (I), a cryogenically controlled 3D Paul trap coupled to a TOFMS (II), and a magnetic-bottle TOF photoelectron analyzer (III). Key parts of the instruments are numbered in Fig. 1 and described in detail as follows.

### A. The electrospray ionization source and the quadruple mass filter system

The ESI syringe (1), syringe pump, and desolvation capillary (2) are similar to our previous designs in the room temperature instrument.[1] Ions produced from the desolvation capillary (2) pass through a 1.5 mm diameter skimmer and enter an octopole ion guide (3). After passing through a second 1.5 mm diameter skimmer, ions are focused by a set of aperture lens into a quadruple mass filter (4). The ions are then deflected by a 90° ion bender (5) either to a channeltron detector (6) to take mass spectra of pristine ions coming from the ESI source or to the 3D Paul trap (9) through a second octopole ion guide (7) and a set of focusing lens (8). This second octopole ion guide (7) is critical for transporting weakly bound ions and solvated species into the Paul trap (9). A bellows is used to house the quadruple mass filter (4) for alignment purposes. Typical working pressures are 1.0 Torr, 10 mTorr, and $4\times10^{-6}$ Torr in the desolvation capillary (2), ion guide (3), and QMS (4) chambers, which are differentially pumped by a mechanical, a blower, and a diffusion pump, respectively.

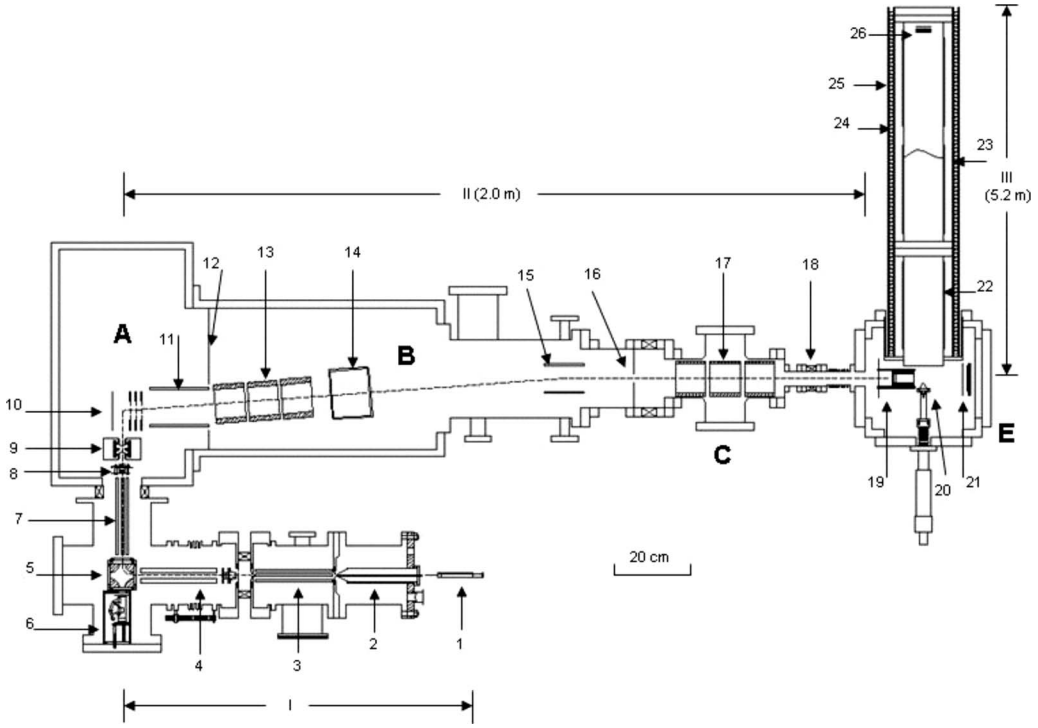


FIG. 1. Schematic view of the second generation low-temperature electrospray PES instrument: (1) syringe, (2) heated desolvation capillary, (3) octopole ion guide, (4) quadruple mass filter, (5) quadruple ion bender, (6) channeltron charged particle detector, (7) octopole ion guide, (8) aperture lens, (9) cryogenically controlled ion trap (see Fig. 2), (10) modifed Wiley–McLarren extraction stack, (11 and 15) horizontal ion deflectors, (12 and 16) apertures, (13 and 17) Einzel lens, (14) vertical ion deflector, (18) gate valve, (19) three-grid mass gate and momentum decelerator assembly, (20) permanent magnet (Nd–Fe–B), (21) 40 mm dual MCP in-line ion detector, (22) heating tape for baking, (23) heat insulation layer, (24) low-field copper solenoid, (25) double-layer $\mu$-metal shielding, and (26) 40 mm $z$-stack MCP photoelectron detector. Note that the octople ion guide (3 and 7) and the quadruple mass filter system (4–6) are customer designed from Extrel CMS (Pittsburgh, PA).

### B. Temperature-controlled ion trap

The heart of the instrument is the temperature-controlled 3D Paul trap (9), where ions are accumulated and cooled. Figure 2 shows the detailed design of the low-temperature ion trap assembly, where key parts are labeled. The 3D Paul trap (R. M. Jordan Company, CA) is attached to the cold head (second stage) of a two-stage closed cycle helium refrigerator (DE204, Advanced Research System) via an extension (b) and an adapter (c) made of oxygen-free high purity copper (OFHC). A 1 mm thick sapphire plate (d) with good thermal conductivity is inserted between the ion trap and the OFHC adapter to electrically isolate the ion trap from ground. The ion trap is enclosed in a gold-coated copper cylinder (g) for thermal shielding, which is connected to the first stage of the helium refrigerator operated at 50 K. Two 2.5 cm diameter holes are cut on the copper cylinder for ion entrance and exit from the Paul trap. The cryostat with the ion trap assembly is mounted on the top of the vacuum chamber via a stainless steel bellows system for alignment.

The lowest ion trap temperature achieved is 10 K, measured by a silicon diode thermal couple (h), which is attached to the OFHC adapter. The temperature can be controlled from 10 to 350 K via a feedback heating system powered by a temperature controller (Model 331, Lake Shore Cryotronics). The background gas is precooled to 50 K by winding the gas line [1.6 mm diameter polyether ether ketone (PEEK) tubing] around the first stage (a) of the cryostat before being fed into the ion trap via a 1.6 mm diameter hole on the alumina spacer in the ion trap assembly. The flow rate

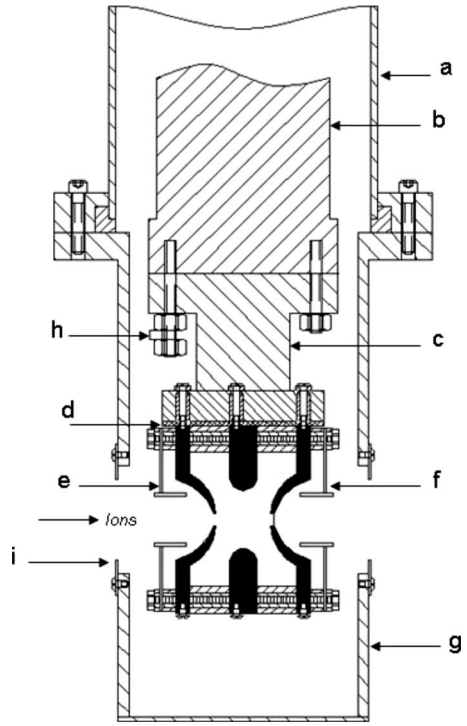


FIG. 2. Schematic view of the cryogenically controlled ion trap assembly: (a) copper thermal shielding cylinder connected to the first stage of the closed cycle helium refrigerator, (b) oxygen-free high purity copper extension connected to the second stage of the closed cycle helium refrigerator, (c) OFHC adapter, (d) 1 mm thick sapphire plate, (e) entrance tube lens, (f) exit tube lens, (g) gold-coated copper shielding, (h) silicon diode thermal couple (model DT-670B-SD, Lake Shore Cryotronics, Inc., Westerville, OH), and (i) entrance aperture lens or beam stopper. The ion trap is a commercial unit from R. M. Jordan Co. (Grass Valley, CA).

of the background gas is controlled by a needle valve. We typically use 0.1 to 1 mTorr helium with 20% $H_2$ as the collision gas in the ion trap for temperatures below 70 K or 0.1–1 mTorr $N_2$ gas for temperatures above 70 K. The background pressure in the ion trap cannot be directly measured, but is estimated from the conductance out of the ion trap and the pressure increase in the vacuum chamber (A in Fig. 1) housing the ion trap assembly.

A pair of entrance and exit tubing lens (e and f) are used to focus incoming ions into the Paul trap and refocus them after being ejected out of the trap into the TOF extraction stack (10). Ions are ejected out of the Paul trap at a 10 Hz repetition rate, giving about 100 ms accumulation and cooling time. A 100 V voltage pulse with a variable time width ($\Delta t$, typically 20 ms) can be applied to the ion trap entrance aperture lens (i) to stop ion loading for a time period ($\Delta t$) before the ions are ejected into the TOFMS (10). Thus ions are trapped and cooled usually for a period of 20–100 ms, during which they experience on average about 2000–10 000 collisions with the background gas.

### C. Time-of-flight mass spectrometer

The linear TOFMS consists of a modified Wiley–McLarren extraction stack (10), similar to our previous design.[1] The addition of a short free-flight zone between the extraction and acceleration stages allows a reasonable mass resolution for a large extraction volume.[43] The ions are ejected from the trap by applying bipolar pulsed voltages on the two end caps (−50 V on the entrance end cap and +30 V on the exit end cap) of the Paul trap, giving an average kinetic energy of ~10 eV for the ejected ions. A 1 kV high voltage pulse is used to perpendicularly extract the ions for TOF mass analyses in a 2 m long flight tube. The ions are focused by two Einzel lens (13 and 17), steered by two horizontal (11 and 15) and one vertical (14) deflectors, and detected by a set of dual microchannel plate (MCP) detector (21). The whole TOFMS flight tube is differentially pumped by a 2000 l/s diffusion pump for the A chamber (base pressure of $1\times10^{-7}$ Torr), a 4000 l/s diffusion pump for the B chamber (base pressure of $5\times10^{-8}$ Torr), a 500 l/s Turbo pump for the C six-way cross (base pressure of $2\times10^{-10}$ Torr), and a 2000 l/s cryopump for the E chamber (base pressure of $8\times10^{-11}$ Torr). The working pressures increase by about one order of magnitude to $1\times10^{-6}$, $2\times10^{-7}$, $5\times10^{-8}$, and $5\times10^{-9}$ Torr in the A, B, C, and E chambers, respectively.

### D. Magnetic-bottle photoelectron analyzer

The magnetic-bottle photoelectron analyzer is also similar to our previous design,[1] except with a longer flight tube (5.2 m) for better resolution for fast electrons. A three-grid mass gate and a subsequent ten-plate deceleration stack (19) are designed to first select an anion of interest and then decelerate it by momentum deceleration to minimize the Doppler broadening, as described in detail previously.[44] A Nd–Fe–B permanent magnet (2.5 cm diameter ×2.5 cm height) machined with a tapered angle (between 60° and 90°) to a sharp tip is mounted on a translation stage (20). The low magnetic field (~10 G) for the magnetic bottle is generated by a solenoid (24) along the 5.2 m long electron flight tube, which is also shielded from the earth field by a double-layer $\mu$-metal cylinder (25). The magnetic field at the tip surface of the permanent magnet is about 1000 G and reduces to ~800 G 5 mm away from the tip in the interaction zone. The magnet is moved further away from the interaction zone to about 1.5 cm for high photon energy detachment lasers (>4 eV) to reduce background electrons from scattered photons. Two lasers are available for photodetachment, a Nd doped yttrium aluminum garnet laser with all its four harmonics (1.06 $\mu$m, 532, 355, and 266 nm) and an excimer laser for 193 nm (ArF) and 157 nm (F2). Photodetached electrons are collected with nearly 100% efficiency by the magnetic bottle and are guided by the low magnetic field along the 5.2 m long electron flight tube. They are detected by a fast $z$-stack detector consisting of a set of three MCPs (26) (R. M. Jordan Co., CA). The C and E chambers and the electron flight tube can be baked *in situ* up to 100 °C by the outside heating tapes (22) to achieve the ultrahigh vacuum base pressures.

### E. Overall operation procedure

The electrospray solution is loaded into the syringe (1), and a −2.2 kV high voltage is usually applied to the stainless steel needle. Negatively charged droplets from the syringe are fed into the 0.75 mm diameter desolvation capillary (2) typically heated to ~80 °C. Anions produced upon desolvation pass through the first skimmer and the octopole ion guide (3). This skimmer is normally biased at −5 V to define the initial ion kinetic energy. After passing through the second skimmer, the anions are focused into the quadruple mass filter (4) and are normally analyzed first by the channeltron detector (6) after the 90° ion bender (5). This analysis is used to optimize the conditions and alignment of the ESI source. Then, all anions are bent toward the Paul trap through the second octopole ion guide (7) for accumulation and cooling.

A transistor-transistor logic signal, which defines the time zero ($T_0$) and initiates the experimental cycle, triggers off the rf voltage on the ring electrode of the Paul trap. After a 2 $\mu$s delay, the cooled ions are ejected out of the trap by applying −50 and 30 V bipolar voltage pulses with 20 $\mu$s duration on the entrance and exit end caps, respectively. The ejected ions are focused by the exit tube lens (f in Fig. 2) into the modified Wiley–McLarren extraction stack (10). After a delay time ($T_3$) relative to the bipolar ion ejection pulse, a 1 kV high voltage pulse is switched on to extract the ions perpendicularly into the 2 m long TOFMS flight tube. For $I^-$ ($m/z$=127), the typical $T_3$ delay time is 21 $\mu$s, which is the ion flight time from the Paul trap to the center of the Wiley–McLarren extraction stack. The TOF for $I^-$ is 62 $\mu$s with a 1 kV extraction voltage. For a given $T_3$, the recorded TOF mass spectrum represents only a narrow mass range due to the fact that ions with different $m/z$ ratios will arrive at the Wiley–McLarren extraction stack at different times. The $T_3$ delay time has to be tuned and optimized for different mass ranges. The experiment is usually performed at a 10 Hz repletion rate, and the whole experimental cycle and delays

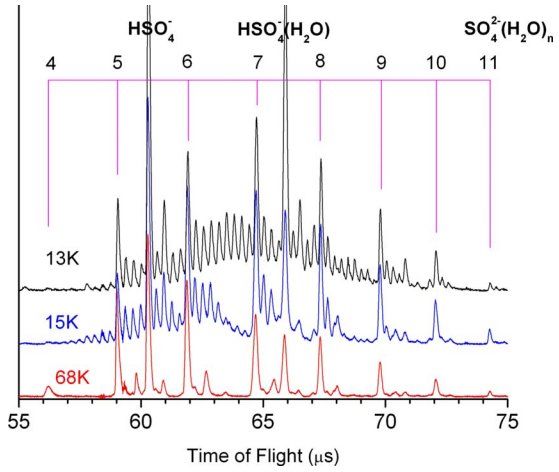


FIG. 3. (Color online) TOF mass spectra of hydrated sulfate clusters taken at three ion trap temperatures with 0.1 mTorr helium background gas with 20% $H_2$. The unlabeled weak peaks in the 68 K spectrum are due to $SO_4^{2-}(H_2O)_m(CH_3CN)$. The additional peaks at 15 and 13 K are due to $H_2$-physisorbed complexes.

are controlled by DG535 pulse generators from Stanford Research Systems. The timing sequence is similar to that described in detail in Ref. 1.

For PES experiments, the ion of interest is first selected by the three-grid mass gate (19) and then decelerated by the momentum decelerator. Details of the mass gate and momentum deceleration have been described previously.[44] A detachment laser beam intercepts the decelerated anions in front of the tip of the permanent magnet in the interaction zone. The detachment laser is operated at a 20 Hz repetition rate with the ion beam off on alternate shots for background subtraction. The photodetached electrons are collected with nearly 100% efficiency by the magnetic bottle and analyzed in the 5.2 m long electron flight tube. Photoelectron TOF spectra are collected and then converted to kinetic energy spectra, calibrated by the known spectra of $I^-$, $OsCl_6^{2-}$, or $ClO_2^-$.[11,45] The electron binding energy spectra are obtained by subtracting the kinetic energy spectra from the detachment photon energy used.

## IV. PERFORMANCE OF THE LOW-TEMPERATURE INSTRUMENT

The initial construction of the low-temperature instrument was finished in late 2004. Since then cold PES spectra of a variety of anions have been obtained and reported[46–64] while we were debugging and making further improvements to this fairly complex instrument. The effects of temperature on the quality of the obtained PES data are dramatic. Moreover, temperature-dependent studies have been made possible, allowing observations of conformation changes of complex anions as a function of temperature.

### A. The time-of-flight mass spectrometer and ion cooling

Figure 3 shows the TOF mass spectra of solvated sulfate dianions at three different temperatures by spraying a 1 mM solution of $(NBu_4)_2SO_4$ in a $H_2O/CH_3CN$ mixed solvent (1/3 volume ratio). The best resolution achieved for the

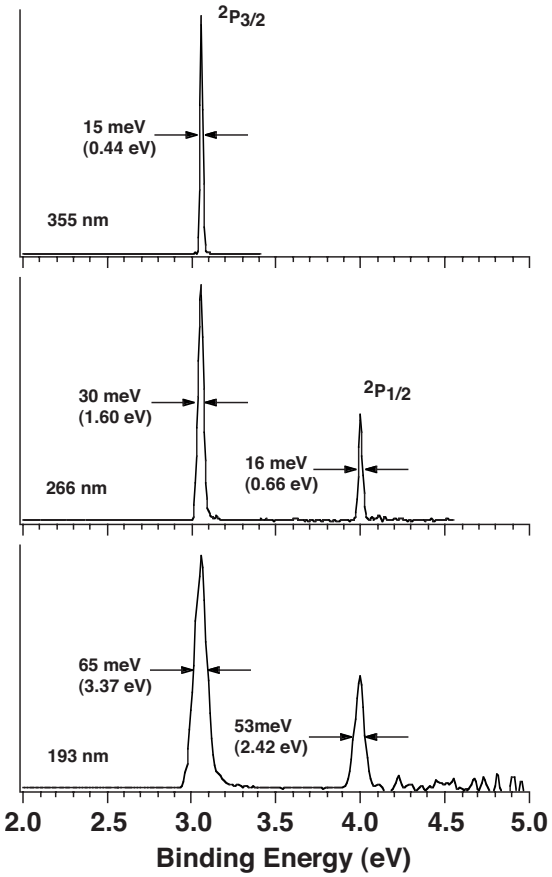


FIG. 4. Photoelectron spectra of $I^-$ at 355 nm (3.496 eV), 266 nm (4.661 eV), and 193 nm (6.424 eV) used for calibrations. The peak widths (FWHM) and their corresponding electron kinetic energies are given.

TOFMS is $M/\Delta M=500$. The background gas used in the Paul trap is ~0.1 mTorr helium with 20% $H_2$. The mass spectrum at 68 K is similar to that at room temperature:[65] besides the strong $HSO_4^-$ and $HSO_4^-(H_2O)$ signals, the solvated sulfate clusters $SO_4^{2-}(H_2O)_n$ ($n=4-11$) are the dominated anions. The weaker peaks in between are due to mixed solvent clusters: $SO_4^{2-}(H_2O)_m(CH_3CN)$.

However, at 15 K trapping temperature, numerous additional peaks separated by $1m/z$ are observed. These additional peaks turned out to be due to condensation of $H_2$ onto the cold anions, i.e., $H_2$-physisorbed clusters. At 13 K, more extensive $H_2$ condensation is observed. The $H_2$ adducts disappear at trapping temperatures above 25 K. Even though the absolute temperatures of the anions cannot be directly measured, the observation of $H_2$ condensation and its temperature dependence suggests that the internal temperatures of the trapped ions should be in close thermal equilibrium with the wall of the ion trap.

### B. Magnetic-bottle photoelectron spectrometer

The performance of the new magnetic-bottle photoelectron spectrometer is similar to that of the previous room temperature instrument,[1] except that the longer electron flight tube yields better resolution for fast electrons. Figure 4 shows the PES spectra of $I^-$ at three photon energies (355, 266, and 193 nm), where the peak width and the corresponding photoelectron kinetic energies are given. The spectral

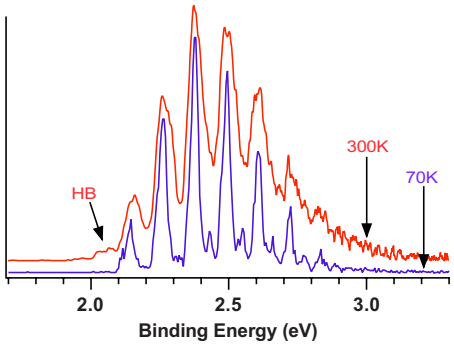


FIG. 5. (Color online) Photoelectron spectrum of $ClO_2^-$ at 355 nm and at 300 K compared to that at 70 K. HB represents hot band transitions.

resolution, measured as full width at half maximum (FWHM), exhibits a strong dependence on the electron kinetic energies. Compared to the same spectra taken with our previous room temperature ESI-PES apparatus,[1] the resolution for fast electrons are indeed improved considerably. For example, the $^2P_{3/2}$ peak at 193 nm defines a spectral resolution of 65 meV FWHM for 3.37 eV electrons, i.e., $\Delta E/E \sim 1.9\%$, relative to 80 meV from the previous apparatus. However, for very low energy electrons, the resolution is slightly inferior in the new instrument. This is probably due to the fact that low energy electrons are more sensitive to local field inhomogeneity that may result from the longer flight tube. For electrons with 1–2 eV kinetic energies, the resolution of the new instrument ($\Delta E/E \sim 1.9\%$) is comparable to the previous instrument. The improvement of fast electrons is important for the study of multiply charged anions, for which high energy electrons often result because of the repulsive Coulomb barrier.[2–9]

### C. Low-temperature photoelectron spectroscopy: Elimination of vibrational hot bands

One major motivation to conduct PES on cold anions is to eliminate vibrational hot bands that cause spectral congestions. Supersonic expansion has been used effectively for cooling neutral molecules for spectroscopic studies, but it is more challenging for ionic species. We demonstrate vibrational cooling in the Paul trap using two examples, one simple anion $ClO_2^-$ and one large anion $C_{60}^-$, as shown in Figs. 5 and 6, respectively. We have used these anions as testing cases to tune cooling conditions, such as the background gas pressure and ion trap operation conditions. We

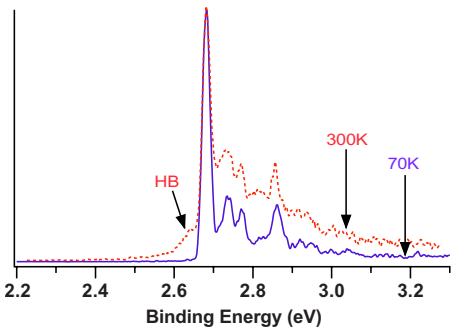


FIG. 6. (Color online) Photoelectron spectrum of $C_{60}^-$ at 355 nm and at 300 K compared to that at 70 K. HB represents hot band transitions.

have found that molecular gases such as $H_2$ and $N_2$ are more effective for vibrational cooling in our ion trap than pure rare gases, most likely due to more effective collisional vibrational-to-vibrational energy transfers. For rigid molecules like $ClO_2^-$ and $C_{60}^-$, there are no low frequency vibrational modes. In these cases, we find that hot vibrational bands can be eliminated at operating temperatures of 70 K or even higher, for which we can simply use $N_2$ as the background gas. For experiments at temperatures lower than 70 K, we usually use helium with 20% $H_2$ as the cooling gas.

The spectra of both $ClO_2^-$ and $C_{60}^-$ were obtained using 0.1 mTorr $N_2$ as the background gas. In the case of $ClO_2^-$, the room temperature spectrum is considerably broadened due to vibrational excitations in the anions. As shown in a previous high resolution study by Gilles *et al.*,[45] the main vibrational progression in the $ClO_2^-$ spectrum is due to the Cl–O symmetric stretching mode. At 70 K, the hot band is completely eliminated, resulting in a much better resolved spectrum under the same electron energy resolution. In particular, the bending mode (weak peaks in between the intense stretching vibrational peaks) can be clearly resolved at 70 K. Even though the spectral resolution is not very high in the current magnetic-bottle instrument, the spectral information in the low-temperature data of $ClO_2^-$ is similar to that obtained in the high resolution spectrum by Gilles *et al.*

$C_{60}^-$ is a large anion, and it carries about 1 eV internal energy at room temperature, as revealed in the long tail in the low binding energy side in the room temperature spectrum.[66] Such a large molecule would have been difficult to be cooled internally even in an intense supersonic expansion. As shown in Fig. 6, the vibrational hot bands are completely eliminated at 70 K for $C_{60}^-$,[47] demonstrating the effectiveness of vibrationally cooling in the Paul trap.

### D. Temperature-dependent photoelectron spectroscopy: Probing conformation changes as a function of temperature

One of the major advantages of using the closed cycle helium refrigerator is the ability to control ion temperatures over a wide temperature range (10–350 K) using a feedback heating system. This capability allows temperature-dependent studies to probe conformation changes and entropic effects in complex anions as a function of temperature. The monocarboxylate anions, $CH_3(CH_2)_nCO_2^-$ ($n$=0–8), were one of the first systems that we studied at low temperatures.[46] Significant spectral sharpening and reduction of vibrational hot bands were observed in the low-temperature spectra for the shorter chain species of $n$=0–4. However, for those species with $n$=5–8, we observed surprisingly a systematic spectral shift to higher binding energies at low temperatures relative to spectra taken at room temperature. The blueshift turned out to be due to a linear to cyclic conformation change at low temperatures, where the negative charge on the carboxylate forms a weak C–H···O hydrogen bond with the terminal $CH_3$ group. Because of the weak strength anticipated for the C–H···O hydrogen bonding, the folded conformation can only be observed at low temperatures due to the large entropic contributions for the linear structure at higher temperatures. Figure 7 displays a

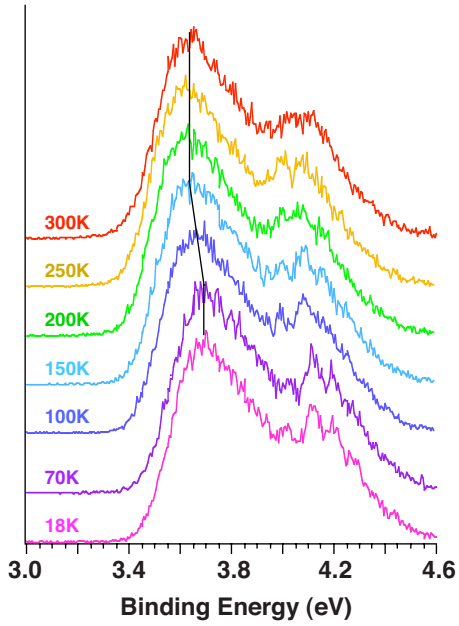


FIG. 7. (Color online) Temperature-dependent photoelectron spectra of $CH_3(CH_2)_6CO_2^-$ at 266 nm. The lines drawn are to guide the eyes only. Note the spectral shift to higher binding energies from 150 to 70 K, indicating conformation changes.

set of spectra for $CH_3(CH_2)_6CO_2^-$ from room temperature down to 18 K.[46] It was observed that the conformation change occurs between 150 and 70 K, below which all the anions become cyclic and no significant changes were observed at lower temperatures.

We have recently carried out an extensive temperature-dependent PES study on hydrated suberate dianions, $^-O_2C-(CH_2)_6-CO_2^-(H_2O)_x$ $(x=1-18)$, and probed their structural changes as a function of temperature and degree of hydration.[62] Our previous room temperature study shows that $H_2O$ solvates the two negative charges in the linear suberate dianion separately and alternatively.[67] However, a water-mediated folding transition was observed at $n=16$, in which the two separate solvation centers merge due to enhanced water-water H-bonding interactions. Our recent low-temperature study shows that the folding transition occurs at fewer solvent molecules $(x=14)$ at low temperatures,[62] again due to the entropic effects that favor the linear conformation at higher temperatures. Detailed temperature-dependent studies also revealed a folding barrier and allowed energetic $(\Delta H)$ and thermal dynamic $(\Delta S)$ information to be obtained between the linear and folded conformations.

## V. CONCLUSIONS AND PERSPECTIVES

In conclusion, a second generation electrospray PES instrument with temperature control capability has been developed to investigate complex anions and solution phase species in the gas phase. The critical part of the new instrument is a cryogenically controlled 3D Paul trap used to accumulate and cool anions from an electrospray ion source. The temperatures of trapped ions are controlled via collisions with a background gas. The Paul trap is connected to a closed cycle helium refrigerator, which can be operated from 5 to 400 K. Temperatures as low as 10 K has been achieved at the ion trap and can be tuned through a feedback heating system from 10 to 350 K. Cold ions have been demonstrated by the observation of $H_2$ condensation. Vibrational cooling from both simple and complex anions has been observed, yielding considerably better resolved photoelectron spectra. Temperature-dependent photoelectron spectroscopic studies have revealed conformation changes as a function of temperature and have yielded both energetic and thermodynamic information for complex anions.

Cooling and temperature tuning of ionic species have been very challenging in ion spectroscopy. The current use of a 3D Paul trap is a relatively simple design and may find wide applications in ion spectroscopy. The observation of physisorbed $H_2$-complexes provides new research opportunities to probe the interactions of $H_2$ with ionic species. The $H_2$-complexes can also be conveniently used for action spectroscopy of complex anions. The temperature-controlled ion trap technique may play the same role for creating cold ions as the supersonic beam technique for creating cold neutral molecules. The temperature tunability of the cryogenic ion trap technique is powerful and will be important for distinguishing isomers of weakly bonded species, as well as allowing temperature-dependent conformation changes to be examined for complex anions and biological molecules.

## ACKNOWLEDGMENTS

This work was supported by the U.S. Department of Energy, Office of Basic Energy Sciences, Chemical Science Division and performed at the W. R. Wiley Environmental Molecular Sciences Laboratory (EMSL), a national scientific user facility sponsored by DOE's Office of Biological and Environmental Research and located at Pacific Northwest National Laboratory, operated for the U.S. Department of Energy by Battelle. We are indebted to Dr. S. E. Barlow for numerous discussions and help during the design and construction of this instrument and to Mr. Ken Swanson for his help with the computer interfacing and data acquisition system. We thank Professor D. Gerlich for valuable discussions about ion trapping and cooling and Dr. H. K Woo and Dr. J. Yang for the debugging and operation of the new instrument. The Instrument Design Lab (IDL) of EMSL is gratefully acknowledged for its help with electronics and the Instrument Shop of the College of Sciences of Washington State University, Pullman, WA for its excellent machine job for all the vacuum chambers.

[1] L. S. Wang, C. F. Ding, X. B. Wang, and S. E. Barlow, Rev. Sci. Instrum. **70**, 1957 (1999).
[2] L. S. Wang and X. B. Wang, J. Phys. Chem. A **104**, 1978 (2000).
[3] X. B. Wang, X. Yang, J. B. Nicholas, and L. S. Wang, Science **294**, 1322 (2001).
[4] X. B. Wang, X. Yang, and L. S. Wang, Int. Rev. Phys. Chem. **21**, 473 (2002).
[5] X. B. Wang, C. F. Ding, and L. S. Wang, Phys. Rev. Lett. **81**, 3351 (1998).
[6] L. S. Wang, C. F. Ding, X. B. Wang, and J. B. Nicholas, Phys. Rev. Lett. **81**, 2667 (1998).
[7] C. F. Ding, X. B. Wang, and L. S. Wang, J. Chem. Phys. **110**, 3635 (1999).
[8] X. B. Wang and L. S. Wang, Nature (London) **400**, 245 (1999).
[9] L. S. Wang, Comments Mod. Phys. D **2**, 207 (2001).
[10] X. B. Wang, J. B. Nicholas, and L. S. Wang, J. Chem. Phys. **113**, 10837 (2000).
[11] X. B. Wang and L. S. Wang, J. Chem. Phys. **111**, 4497 (1999).

[12] X. B. Wang and L. S. Wang, J. Am. Chem. Soc. **122**, 2096 (2000).
[13] X. B. Wang, F. E. Inscore, X. Yang, J. J. A. Cooney, J. H. Enemark, and L. S. Wang, J. Am. Chem. Soc. **124**, 10182 (2002).
[14] T. Waters, X. B. Wang, and L. S. Wang, Coord. Chem. Rev. **251**, 474 (2007).
[15] X. B. Wang, S. Niu, X. Yang, S. K. Ibrahim, C. J. Pickett, T. Ichiye, and L. S. Wang, J. Am. Chem. Soc. **125**, 14072 (2003).
[16] S. Niu, X. B. Wang, J. A. Nichols, L. S. Wang, and T. Ichiye, J. Phys. Chem. A **107**, 2898 (2003).
[17] X. Yang, M. Razavet, X. B. Wang, C. J. Pickett, and L. S. Wang, J. Phys. Chem. A **107**, 4612 (2003).
[18] X. Yang, S. Q. Niu, T. Ichiye, and L. S. Wang, J. Am. Chem. Soc. **126**, 15790 (2004).
[19] X. Yang, X. B. Wang, E. R. Vorpagel, and L. S. Wang, Proc. Natl. Acad. Sci. U.S.A. **101**, 17588 (2004).
[20] C. Tard, X. Liu, S. K. Ibrahim, M. Bruschi, L. D. Gioia, S. Davies, X. Yang, L. S. Wang, and C. J. Pickett, Nature (London) **433**, 610 (2005).
[21] J. Q. Searcy and J. B. Fenn, J. Chem. Phys. **61**, 5282 (1974).
[22] R. E. Smalley, L. Wharton, and D. H. Levy, Acc. Chem. Res. **10**, 139 (1977).
[23] S. Goyal, D. L. Schutt, and G. Scoles, Phys. Rev. Lett. **69**, 933 (1992).
[24] M. Hartmann, R. E. Miller, J. P. Tonennies, and A. Vilesov, Phys. Rev. Lett. **75**, 1566 (1995).
[25] K. Nauta and R. E. Miller, Science **283**, 1895 (1999).
[26] W. H. Robertson, J. A. Kelly, and M. A. Johnson, Rev. Sci. Instrum. **71**, 4431 (2000).
[27] W. H. Robertson and M. A. Johnson, Annu. Rev. Phys. Chem. **54**, 173 (2003).
[28] D. Gerlich, Adv. Chem. Phys. **82**, 1 (1992).
[29] D. Gerlich and S. Horning, Chem. Rev. (Washington, D.C.) **92**, 1509 (1992).
[30] Y. S. Wang, C.-H. Tsai, Y. T. Lee, H.-C. Chang, J. C. Jiang, O. Asvany, S. Schlemmer, and D. Gerlich, J. Phys. Chem. A **107**, 4217 (2003).
[31] D. J. Douglas and J. B. French, J. Am. Soc. Mass Spectrom. **3**, 398 (1992).
[32] A. V. Tolmachev, H. R. Udseth, and R. D. Smith, Rapid Commun. Mass Spectrom. **14**, 1907 (2000).
[33] X. Guo, M. Duursma, A. Al-Khalili, L. A. McDonnell, and R. M. A. Heeren, Int. J. Mass. Spectrom. **231**, 37 (2004).
[34] S. Guan, H. S. Kim, A. G. Marshall, M. C. Wahl, T. D. Wood, and X. Xiang, Chem. Rev. (Washington, D.C.) **94**, 2161 (1994).
[35] S. Schlemmer, A. Luca, J. Glosik, and D. Gerlich, J. Chem. Phys. **116**, 4508 (2002).
[36] O. V. Boyarkin, S. R. Mercier, A. Kamariotis, and T. R. Rizzo, J. Am. Chem. Soc. **128**, 2816 (2006).
[37] J. Zhou, D. T. Moore, L. Wöste, G. Meijer, D. M. Neumark, and K. R. Asmis, J. Chem. Phys. **125**, 111102 (2006).
[38] S. M. Michael, M. Chien, and D. M. Lubman, Rev. Sci. Instrum. **63**, 4277 (1992).
[39] R. W. Purves and L. Li, J. Am. Soc. Mass Spectrom. **8**, 1085 (1997).
[40] J. F. J. Todd, Mass Spectrom. Rev. **10**, 3 (1991).
[41] J. H. Parks, S. Pollack, and W. Hill, J. Chem. Phys. **101**, 6666 (1994).
[42] S. Pollack, D. Cameron, M. Rokni, W. Hill, and J. H. Parks, Chem. Phys. Lett. **256**, 101 (1996).
[43] W. A. de Heer and P. Milani, Rev. Sci. Instrum. **62**, 670 (1991).
[44] L. S. Wang, H. S. Cheng, and J. Fan, J. Chem. Phys. **102**, 9480 (1995).
[45] M. K. Gilles, M. L. Polak, and W. C. Lineberger, J. Chem. Phys. **96**, 8012 (1992).
[46] X. B. Wang, H. K. Woo, B. Kiran, and L. S. Wang, Angew. Chem., Int. Ed. **44**, 4968 (2005).
[47] X. B. Wang, H. K. Woo, and L. S. Wang, J. Chem. Phys. **123**, 051106 (2005).
[48] X. B. Wang, B. Dai, H. K. Woo, and L. S. Wang, Angew. Chem., Int. Ed. **44**, 6022 (2005).
[49] H. K. Woo, X. B. Wang, L. S. Wang, and K. C. Lau, J. Phys. Chem. A **109**, 10633 (2005).
[50] X. B. Wang, H. K. Woo, B. Kiran, and L. S. Wang, J. Phys. Chem. A **109**, 11089 (2005).
[51] H. K. Woo, X. B. Wang, B. Kiran, and L. S. Wang, J. Phys. Chem. A **109**, 11395 (2005).
[52] T. Waters, H. K. Woo, X. B. Wang, and L. S. Wang, J. Am. Chem. Soc. **128**, 4282 (2006).
[53] X. B. Wang, H. K. Woo, L. S. Wang, B. Minofar, and P. Jungwirth, J. Phys. Chem. A **110**, 5047 (2006).
[54] X. B. Wang, H. K. Woo, X. Huang, M. M. Kappes, and L. S. Wang, Phys. Rev. Lett. **96**, 143002 (2006).
[55] H. K. Woo, X. B. Wang, K. C. Lau, and L. S. Wang, J. Phys. Chem. A **110**, 7801 (2006).
[56] T. Waters, X. B. Wang, H. K. Woo, and L. S. Wang, Inorg. Chem. **45**, 5841 (2006).
[57] T. Waters, X. Huang, X. B. Wang, H. K. Woo, R. A. J. O'Hair, A. G. Wedd, and L. S. Wang, J. Phys. Chem. A **110**, 10737 (2006).
[58] X. B. Wang, Y. L. Wang, H. K. Woo, J. Li, G. S. Wu, and L. S. Wang, Chem. Phys. **329**, 230 (2006).
[59] H. K. Woo, K. C. Lau, X. B. Wang, and L. S. Wang, J. Phys. Chem. A **110**, 12603 (2006).
[60] B. Jagoda-Cwiklik, X. B. Wang, H. K. Woo, J. Yang, G. J. Wang, M. F. Zhou, P. Jungwirth, and L. S. Wang, J. Phys. Chem. A **111**, 7719 (2007).
[61] X. B. Wang, H. K. Woo, J. Yang, M. M. Kappes, and L. S. Wang, J. Phys. Chem. C **111**, 17684 (2007).
[62] X. B. Wang, J. Yang, and L. S. Wang, J. Phys. Chem. A **112**, 172 (2008).
[63] J. Yang, X. P. Xing, X. B. Wang, L. S. Wang, A. P. Sergeeva, and A. I. Boldyrev, J. Chem. Phys. **128**, 091102 (2008).
[64] X. B. Wang, K. Matheis, I. N. Ioffe, A. A. Goryunkov, J. Yang, M. M. Kappes, and L. S. Wang, J. Chem. Phys. **128**, 114307 (2008).
[65] X. Yang, X. B. Wang, and L. S. Wang, J. Phys. Chem. A **106**, 7607 (2002).
[66] X. B. Wang, C. F. Ding, and L. S. Wang, J. Chem. Phys. **110**, 8217 (1999).
[67] X. Yang, Y. J. Fu, X. B. Wang, P. Slavicek, M. Mucha, P. Jungwirth, and L. S. Wang, J. Am. Chem. Soc. **126**, 876 (2004).